ORIGINAL PAPER

CrossMark

Microring resonator-based photonic system for terahertz signal generation

Rohan Katti[1] · Shanthi Prince[1]

Abstract
We propose a photonic system based on add–drop microring resonator and mode-locked laser for terahertz (THz) signal generation. A mode-locked laser acts as an input source to the microring resonator. The transfer characteristics of the microring resonator generate Lorentzian shaped pulses at the output ports of the microring resonator. These series of pulses obtained are then investigated in two approaches; in the first approach, the output of the microring resonator is given to a photodetector which generates 33 THz pulses separated by a spacing of 1 THz with a full width at half maximum (FWHM) of 0.15 THz. In the second approach, the output of the microring resonator is given to an optical filter to extract a particular frequency component. In this case, a single THz carrier with a FWHM of 0.2618 THz is obtained. The THz frequency components generated by the proposed photonic system can act as carriers for communication between the indoor user and the base station of a pico/femto cell in a 5G environment.

Keywords Microwave photonics · THz signal generation · Microring resonator · Frequency comb generation · Mode-locked laser

1 Introduction

Microwave photonics (MWP) is an amalgamation of two different domains of radio frequency and fiber optics. It deals with the study of photonic devices which operate at microwave frequencies. It has received a great thrust in the research community as it has been pointed out that microwave photonics is capable of providing viable solutions in realizing complex functionalities in microwave domain [1–4]. The frequency range associated with the field of microwave photonics spans from few kilohertz (KHz) of the radio frequency (RF) domain to few hundred's of terahertz (THz). The main reason for the origin of this field was to address the problems faced by the researchers working in RF domain while venturing into optical domain [5]. Although the interaction between optics and microwaves has been studied for many years, the term 'Microwave Photonics' was coined

in 1991, and it was anticipated that this merger of microwaves and photonics would provide a novel approach and solutions to future fiber-radio systems [6]. As anticipated, microwave photonics, today is a mature interdisciplinary area of research with immense research contributions. There is a remarkable progress in this field, and the research contributions seem to grow drastically. There are numerous advantages which the microwave photonic links extend when compared to traditional electronic links such as reduction in size, weight and cost, less attenuation and dispersion, immune to electromagnetic interference and large capacity to transfer high data rate signals [3]. Microwave photonics incorporates these advantages offered by photonic technologies to generate, process, distribute and analyze microwave and millimeter (mmWave) signals [7]. Microwave photonics has made its mark in diverse range of applications which include broadband wireless access and transport networks [8, 9], satellite communications [10], distributed antenna systems [11], optical signal processing [12], medical imaging [13], electronic warfare systems [14].

With the ever-increasing capacity crunch and demands for data rates and bandwidth, contribution of photonics in terms of compact, low-power devices with wide range of tunability makes microwave photonics a favorable option to address

✉ Rohan Katti
rohankatti23@gmail.com

Shanthi Prince
shanthi.p@ktr.srmuniv.ac.in

[1] Department of ECE, SRM Institute of Science and Technology, SRM Nagar, Kattankulathur, Tamil Nadu 603203, India

the challenges and complexities of 5G technology [15, 16]. The domain of microwave photonics is seen as a potential candidate for addressing the challenges of upcoming technologies such as 5G and terahertz systems. The architecture of a 5G network will consist of many pico and femto cells with a dedicated base station to serve the ever-increasing number of connected devices. These wireless access networks which are expected to handle multiple gigabits of data rates and also billions of connected devices will be the driving force for microwave photonics to offer potential solutions for the challenges posed by 5G networks. The total allocated bandwidth of 7–9 GHz for current technologies such as millimeter wave communications is going to limit the total throughput of the channel for the increasing demand [17]. This calls for a new frequency band called terahertz (THz) frequency band which spans between frequencies of 0.1 THz and 10 THz when the bandwidth requirement is few tens of GHz. THz communications are said to play a major role in applications such as fronthaul and backhaul of base stations of femto cells, wireless local and personal area networks for smart offices and smart homes, respectively, near-field communications, wireless communications in data centers, device–device communications [17, 18].

Another distinct feature of THz signals is that they can propagate through nonmetallic components like bags, suitcases, etc. This paves a way for THz imaging to play a crucial role in variety of applications. In compressive sensing, a sparse signal can be sensed on sub-Nyquist sampling rate. A THz image can be considered as a sparse signal, thereby realizing THz imaging systems based on compressive sensing [19]. Compressive sensing techniques based on photonics have been recently proposed based on different methods. Chen et al. [20] have proposed a microring resonator-based filter for photonic compressive sensing. Thus, THz signals can pave a way for novel compressive sensing methods and techniques for numerous applications.

THz signal generation in photonics domain has been extensively studied and reported as it is one of the simplest ways to generate high data rate signals with the help of photonic devices which have large bandwidths [21]. There have been many photonics-based techniques proposed in literature for generating THz signals. Song et al. [22] have proposed a photonic technique based on phase modulator and photomixer for generation of a sub-terahertz signal. A stable mmWave/THz signal is generated by Sun et al. [23] based on dual-heterodyne phase fluctuations. Carpintero et al. [24] have proposed a photonic technique for generation of THz signals based on optical heterodyning. They have realized a polymer waveguide structure which can be tuned by thermal means for generating a 330 GHz signal. A photonic crystal fiber in Mach–Zehnder interferometer structure-based technique is proposed for generating a stable THz emission [25].

Variable and tunable wavelengths with spacing of 0.9 THz, 2.6 THz were generated.

Microring resonators (MRR) are considered to be one of the important building blocks of integrated photonics and have found applications in widespread fields [26, 27]. Microring resonators are considered to be one of the commonly employed photonic devices in integrated microwave photonic applications. Microring resonators-based microwave photonic filters have been demonstrated with infinite impulse response [28]. A silicon-on-insulator microring resonator forms an integral part of a optical temperature sensor based on integrated optoelectronic oscillator [29]. A triple cascaded ring resonator structure is proposed for designing a tunable microwave phase shifter with complete 360° phase shift range [30]. All these examples imply that microring resonators have wide range of applications in the field of microwave photonics. Several works on microring resonator-based photonic techniques for THz signal generation have been proposed in the literature. Amiri et al. [31] have proposed a silicon microring resonator for multi-soliton generation applicable for THz communication. A modified add–drop microring resonator has been proposed for generation of high-capacity THz carrier for RFID applications [32]. Amiri et al. [33] have proposed a microring resonator structure based on ion exchange method for generating dual wavelengths whose spacing is in the range of 0.25–0.96 THz for THz communications, sensing and spectroscopy applications. Sinha et al. [34] have proposed a tunable microring resonator-based THz source which generates THz waves in the range of 0.5–10 THz. A very recent work by Furusawa et al. [35] focuses on THz signal generation based on frequency combs generated by microring resonators. The frequency combs are generated in a microring resonator based on silicon nitride (SiN) waveguide based on Lugiato–Lefever (LL) model. Mu-Chieh et al. [36] have recently proposed mode-locked laser-based photonic integrated circuit for millimeter wave and terahertz carrier generation.

In this paper, we propose a photonic system for THz signal generation based on add–drop microring resonator and mode-locked laser. Generation of a frequency comb at the output of a microring resonator forms the basis of this THz signal generation scheme. The generation of THz signals in the presence of an optical filter after the microring resonator and an electrical filter after the photodetector is investigated. The microring resonator which forms the core element of the THz generation system is modeled in a commercial device modeling tool based on finite difference time domain (FDTD) algorithm. The organization of the paper is as follows, Sect. 2 deals with the architecture of the proposed system for THz signal generation based on microring resonators. Section 3 presents the analysis and simulation results of the proposed photonic system for THz signal generation. Section 4 consists of modeling of microring resonator of proposed dimensions

which is incorporated in the proposed photonic system for THz signal generation. Section 5 concludes the paper.

1.1 Application of THz carriers in a cell densification environment of a 5G network

As 5G is expected to be rolled out in near future, mobile operators have upgraded their networks to long-term evolution (LTE) and LTE advanced and have started planning for 5G. 5G radio network and infrastructure must address the ever-increasing demands for higher mobile bandwidth. Apart from realizing a completely new infrastructure for 5G, upgrades in the 5G network infrastructure also need improvement in the existing infrastructure. In order to accommodate 5G, there is a need to redesign the air interfaces and the radio access networks (RAN). Thus, a new radio (NR) for 5G along with massive multiple-input–multiple-output (MIMO) which will drive distributed antenna systems (DAS) are expected to play a crucial role in deployment of 5G network infrastructure [37]. Another development in the 5G infrastructure is the cloud RAN (C-RAN) where there is a centralized baseband processing unit (BBU) which serves multiple remote radio heads (RRH) [38]. Fronthaul, which is the connection between a RRH and BBU, is changing from conventional coax cables to fiber connections. As far as mobile backhaul is concerned, next-generation passive optical network and carrier Ethernet are the technologies which have replaced the traditional microwave connections. It is also expected that fibers will replace the present Ethernet, high-speed copper cables in order to address the ever-increasing demands of data rates that 5G applications need [37].

It has been observed that a wireless user stays indoor for approximately 80% of the time and outdoor for approximately 20% of the time [39]. A unique feature of 5G architecture is to have distinct setups for indoor and outdoor users such that the indoor user will receive the signal with considerably less penetration loss when compared to the signal received from the base station which is present outside and has to penetrate through walls of the indoor environment [40]. One of the challenges to be addressed in 5G architecture is network densification. In order to offload traffic from the macro cells, small cells have proven to be potential candidates. Small cells which are low-power wireless access points not only help in improving the cellular coverage but also increase the capacity. Small cells can be pico cells which can support around 64–128 users and can be deployed in airports, shopping malls or femto cells which are primarily deployed in residential environments and can support around 4–32 users [41]. A typical macro cell structure illustrating the scenario of small cells is shown in Fig. 1.

Millimeter wave spectrum is considered to be one of the major requirements of 5G mobile networks as they are capable of enabling gigabit per second throughput along with the large bandwidth. Small cells are able to provide various multimedia applications such as high definition television (HDTV), wireless gigabit ethernet as they operate in the mmWave bands such as 28, 38, 71–76 and 81–86 GHz [40]. Apart from the mmWave band, THz band can also be considered for small cell communication. THz band is capable of providing ultra-high-speed data rates with coverage distance of up to 10 m [18]. The communication between the base station of a pico/femto cell and the users or the communication between two different devices present inside same cell or different small cells can take place through a THz link.

Although THz communications opens a door to plethora of applications for 5G and beyond, there are still some challenges which need to be addressed from photonics point of view. Monolithic integration of photonic components plays an important role in the improvement of overall system performance in terms of size and cost. Transmission power is another factor which needs to be addressed. THz transmitters are limited by the responsivity, frequency response of the photomixer. Beamforming, which reduces the power consumption by steering the optimal power to mobile units, is considered to be one of the front runners of 5G. It is still difficult to achieve accurate beam steering capability at higher bandwidths which are required for transmitting data at the rate of Gbps. THz amplifiers can improve the performance of a system over long transmission distances. The cost involved in the integration of THz transistors is also expected to be one of the challenges in improving the THz communication technology [42].

2 Microring resonator-based photonic system for THz signal generation

The proposed system for THz signal generation is investigated in two ways, in the first scenario, a mode-locked laser (MLL) is the input at the input port of the MRR. The output at the drop port of the MRR consists of comb of equally spaced Lorentzian shaped pulses. This frequency comb generated at the drop port of the microring resonator is made to fall on a photodetector. The output of the photodetector is then given to an electrical filter in order to obtain the required frequency component of the THz signals. The block schematic of the proposed system for generating THz signals in this scenario is shown in Fig. 2.

In the second approach, an optical filter is used to filter the comb lines generated at the output of the microring resonator and the filtered spectrum is made to fall on a photodetector. The output of the photodetector gives the electrical spectrum of the generated THz signal which can be visualized on a spectrum analyzer. An electrical filter can be used to remove the noise components present in the signal appearing at the output of the photodetector. The block schematic of the pho-

Fig. 1 Typical cell structure in 5G architecture illustrating the deployment of small cells such as pico/femto cells in a macro cell. *MBS* mobile base station, *PBS* pico cell base station, *FBS* femto cell base station, *D2D* device to device, *mm Wave* millimeter wave
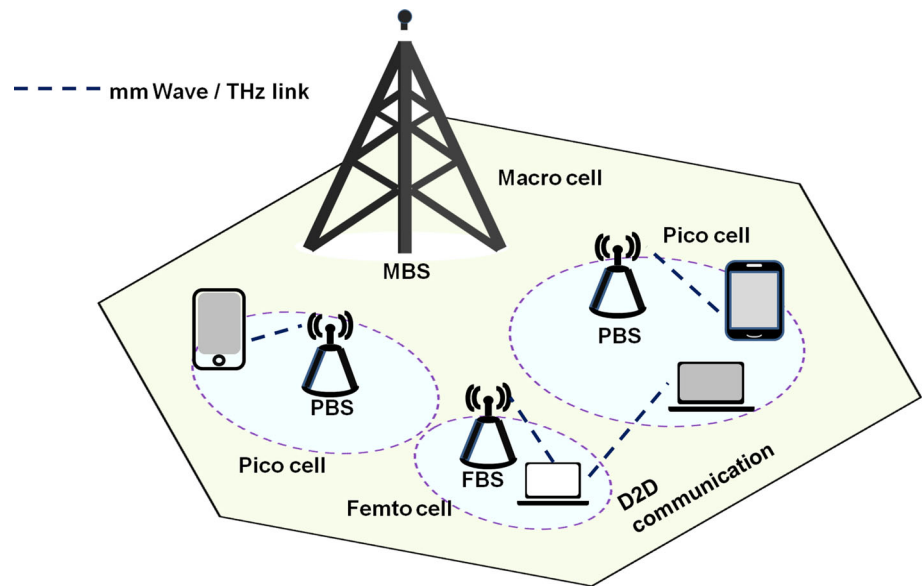

Fig. 2 Block schematic of photonic system for THz generation based on microring resonator and electrical filter
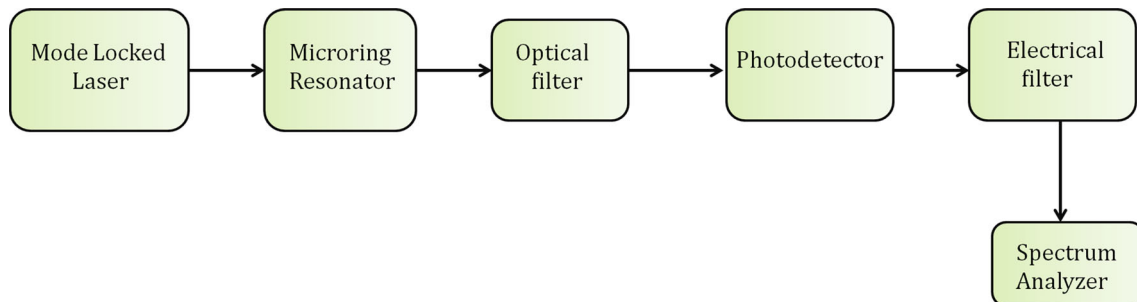

Fig. 3 Block schematic of photonic system for THz generation based on microring resonator and optical filter

tonic system for THz signal generation in the presence of an optical filter is shown in Fig. 3.

The generated THz signals can act as carriers for communication between the pico/femto cell base station and the user present inside a pico/femto cell or between different devices present in the pico/femto cells.

3 Analysis and simulation results of proposed photonic system for THz signal generation

The proposed system for THz signal generation is analyzed mathematically in terms of electric field equations. The sim-

ulation results of the proposed system are also discussed in detail.

3.1 Mathematical analysis of proposed photonic system for THz signal generation

A microring resonator consists of a circular ring cavity coupled to two bus waveguides as shown in Fig. 4. It consists of two input ports namely input port and add port and two output ports namely through port and drop port.

The ring resonator is said to be in resonance if the round trip phase shift introduced in the signal inside the cavity is equal to integer times 2π. If the wavelength of the incoming signal is not a multiple of the optical path length of the round

Fig. 4 Block schematic of a typical microring resonator with the notations of coupling coefficients and electric fields
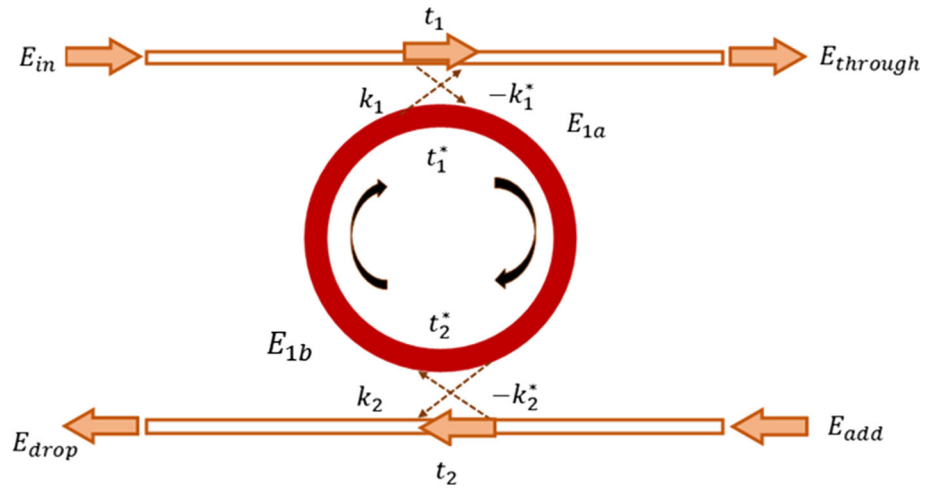
trip, then the resonator is said to be in OFF resonance. The resonance condition of the microring resonator is given as

$$n_{eff} L = m\lambda_{res} \tag{1}$$

where n_{eff} is the effective refractive index of the waveguide, $L(=2\pi r)$ is the circumference of the ring resonator, r being the ring radius, m is an integer which denotes the azimuthal mode number and λ_{res} is the resonant wavelength of the microring resonator.

A mode-locked laser consists of a series of equally spaced frequency components whose phase components have fixed relationship with each other, thereby maintaining a steady-state variation in the output of the MLL which is a function of time [43]. The intensity of the laser beam emerging from a mode-locked laser is the sum of electric fields of all the longitudinal modes of the laser beam and is given by [44]

$$E(t) = \sum_{m=m_{min}}^{m_{max}} E_{0,m} \cos(2\pi \upsilon_m t + \varphi_m) \tag{2}$$

m represents the number of modes, $E_{0,m}$ being the amplitude of the mth laser mode with a phase φ_m and frequency υ_m. The output pulses of a mode-locked laser are generally bell shaped and different functions like Gaussian, sech^2 can be used to represent these pulses. The Gaussian representation of the pulse generated at the output of a mode-locked laser as a function of time can be represented as [44]

$$E_{laser}(t) = E_{laser,0} e^{-2\ln 2(t/\Delta t_{FWHM})^2} e^{i(2\pi \upsilon_m + \beta_{chirp} t)t} \tag{3}$$

where $E_{laser,0}$ represents the electric field of the laser beam with a pulse width of Δt_{FWHM}. The chirp introduced in the pulse is represented by the term i $\beta_{chirp} t$ where the slope of

the chirp is given by β_{chirp}. Assuming a chirp-free Gaussian pulse generated at the output of the MLL, we have

$$E_{laser}(t) = E_{laser,0} e^{-2\ln 2(t/\Delta t_{FWHM})^2} e^{i(2\pi \upsilon_m t)} \tag{4}$$

The electric field at the drop port of the microring resonator is given by [45]

$$E_{drop} = \frac{-k_1^* k_2 \sqrt{\alpha} e^{i\frac{\varphi}{2}}}{1 - t_1^* t_2^* \alpha e^{i\varphi}} E_{in} \tag{5}$$

where t_1, t_2 are the through coupling coefficients at the top and bottom bus waveguides, respectively, k_1, k_2 are the cross-coupling coefficients at the top and bottom bus waveguides, respectively, and * denotes the complex conjugate of that particular coupling coefficient. α represents the loss coefficient of the ring resonator. The round trip phase shift is denoted by φ and is given by $(2\pi \cdot n_{eff} \cdot L)/\lambda$. E_{in}, E_{drop} denote the electric field at the input port and drop port, respectively. It is clear from Figs. 2 and 3 that the output pulses generated by a mode-locked laser are given as input to the microring resonator. Thus, in the proposed system for THz carrier generation, the electric field appearing at the output of the microring resonator is given by

$$E_{drop} = \frac{-k_1^* k_2 \sqrt{\alpha} e^{i\frac{\varphi}{2}}}{1 - t_1^* t_2^* \alpha e^{i\varphi}} E_{laser,0} e^{-2\ln 2(t/\Delta t_{FWHM})^2} e^{i(2\pi \upsilon_m t)} \tag{6}$$

Equation (6) represents the product of the transfer function of the microring resonator and the output intensity of the mode-locked laser. The plot of Eq. (6) results in a train of pulses whose amplitudes decay with time and is shown in Fig. 5.

The values of repetition rate and FWHM of the pulse (Δt_{FWHM}) were taken as 1 THz and 1e−12 m, respectively. It can be inferred from Eq. (6) that, the coupling coefficients are fixed for the microring resonator employed in the proposed

Fig. 5 Generated train of pulses with intensity decaying with time at the output of the MRR when a MLL is the input
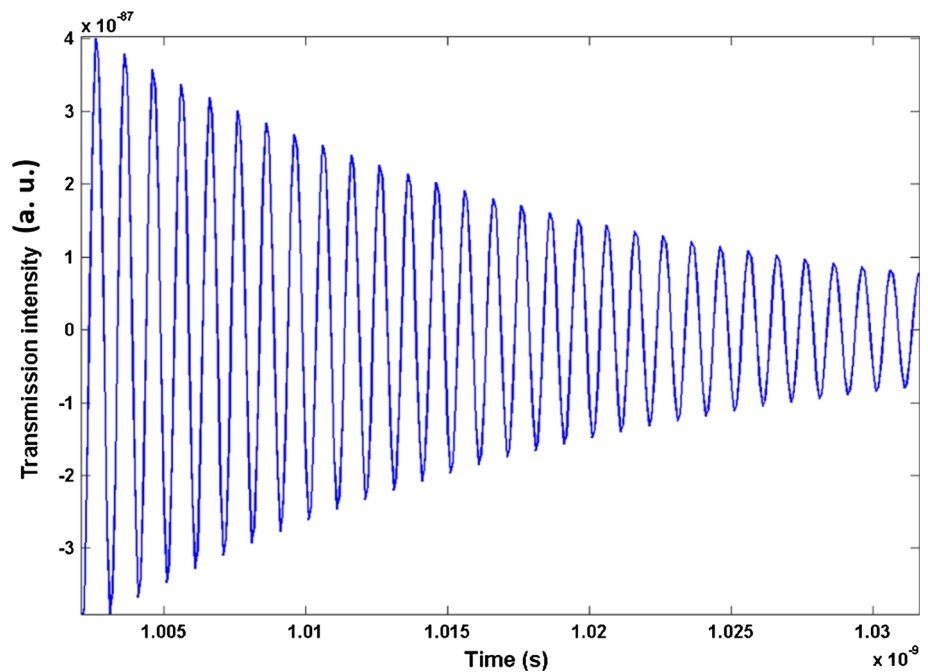
technique for THz carrier generation. A parameter of interest in this analysis is the frequency of the mode υ_m. There have been many techniques proposed in recent years to generate pulses with repetition rates in the order of GHz and THz [46–49]. Higher repetition rate in the order of THz is suitable for generation of THz carriers as it is the only factor present in Eq. (6) which dominates the output waveform. The output of the microring resonator is then given to a photodetector which converts the incident optical frequency comb generated at the output of MRR to its electrical equivalent. The responsivity $\mathcal{R}$ of the photodetector in A/W is then given by

$$\mathcal{R} = \frac{I}{P_0} \tag{7}$$

where P_0 represents the amount of optical power incident on the photodetector and I is the generated photocurrent. Since we know that the optical power is given by the square of the electric field intensity, Eq. (7) can be rewritten as

$$\mathcal{R} = \frac{I}{E_{\text{drop}}^2} \tag{8}$$

The quantum efficiency η of the phototdetector in this case is given by

$$\eta = \mathcal{R}\frac{h\nu}{q} \tag{9}$$

where h is the Planck's constant, q is the charge of the electron and ν is the frequency of the incident optical signal.

Table 1 Parameters used in simulation of photonic system for THz signal generation

Parameter	Value
MLL power	0.5 W
MLL repetition rate	1 Tbps
MLL wavelength	1555.33 nm
Radius of MRR	20 µm
Quantum efficiency of photodetector	0.8
Electrical filter type	Low pass Bessel
Electrical filter bandwidth	10 GHz
Optical filter bandwidth	1 nm

3.2 Simulation results and discussion

The block schematics of the proposed photonic system for THz signal generation are designed and simulated in Rsoft's Optsim tool. Simulation parameters are given in Table 1.

3.2.1 Simulation results of proposed photonic system with MRR and electrical filter

The photonic system for generation of THz signals in the presence of an electrical filter as shown in Fig. 2 is implemented in RSoft Optsim tool. RSoft's Optsim is an advanced and accurate simulation package for design and simulation of optical communication systems at the signal propagation level. The mode of simulation is selected to be steady state.
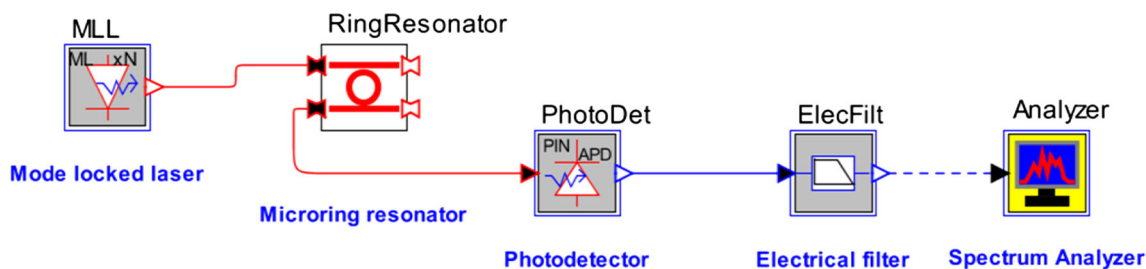
Fig. 6 Implementation of photonic system for THz signal generation in the presence of an electrical filter in RSoft OptSim tool
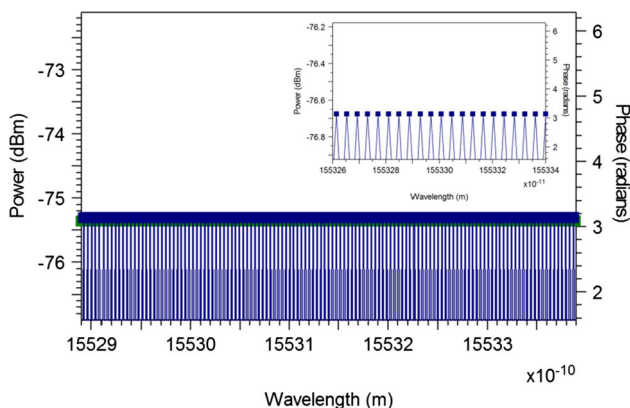

Fig. 7 Spectrum of the mode-locked laser with a repetition rate of 1000 Gbps. Zoomed in version of the spectrum is shown in the inset

The layout of the photonic system with MRR and electrical filter is shown in Fig. 6.

Mode-locked laser (MLL) is used as an optical source to generate bell-shaped optical signals with a repetition rate of 1000 Gbps and FWHM of 1e−12 m. The spectrum of the mode-locked laser is shown in Fig. 7. The wavelength of the MLL is adjusted to the resonance wavelength of the MRR which is 1555.33 nm. The input power is set at 0.5 W.

The output of the MLL is coupled to the input port of the MRR. The Lorentzian shaped transfer function of the MRR is responsible for the generation of a series of pulses at the through port and drop port separated by the free spectral range (FSR). The spectrum of the signals generated at the through port and drop port of the MRR is shown in Fig. 8.

It can be inferred from Fig. 8 that the transmission at the resonance wavelength of 1555.33 nm is low at the through port and high at the drop port. The FSR obtained is 7.5 nm and the full width at half maximum (FWHM) of the pulse is 1.82 nm. The optical power at the output of the MRR is −32.64 dBm. The output of the drop port of the MRR is given to a phototdetector. The input power is varied from 1 mW to 0.5 W; it is observed that the spectrum of the signal at the output of the photodetector is degraded for low input power and starts improving as the input power increases. The spectrum of the signal at the output of the photodetector for various values of input power is shown in Fig. 9.

A series of 33 THz pulses separated by a spacing of 1 THz are obtained at the output of the photodetector. The FWHM of the pulses obtained is 0.15 THz, and the power of the signal is −49.35 dBm. These pulses can be filtered to obtain the required frequency component for the required application. The output of the electrical filter is shown in Fig. 10.
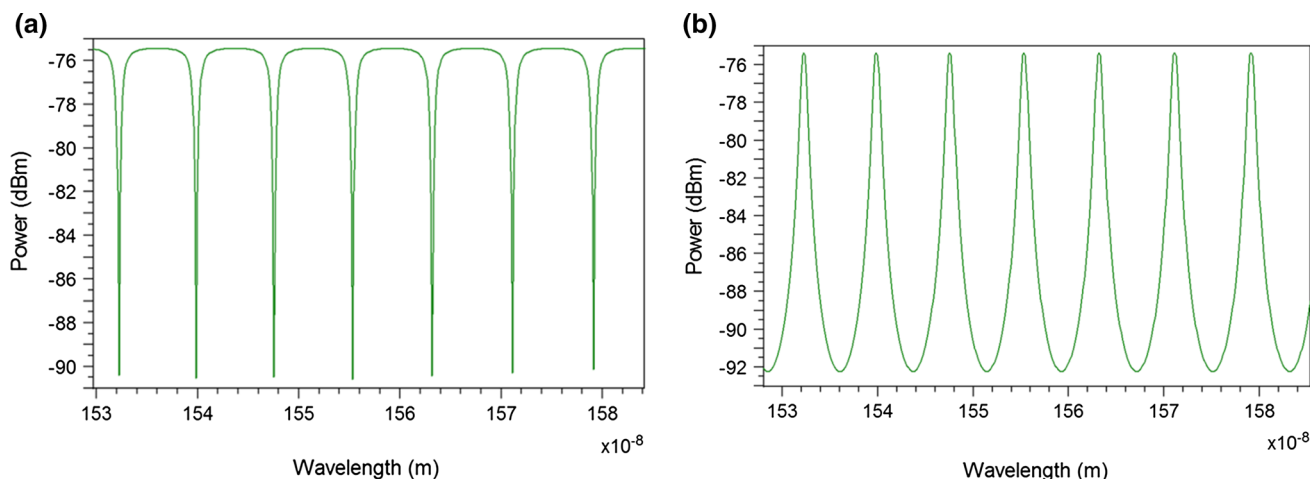

Fig. 8 Transmission spectrum of MRR at **a** through port, **b** drop port
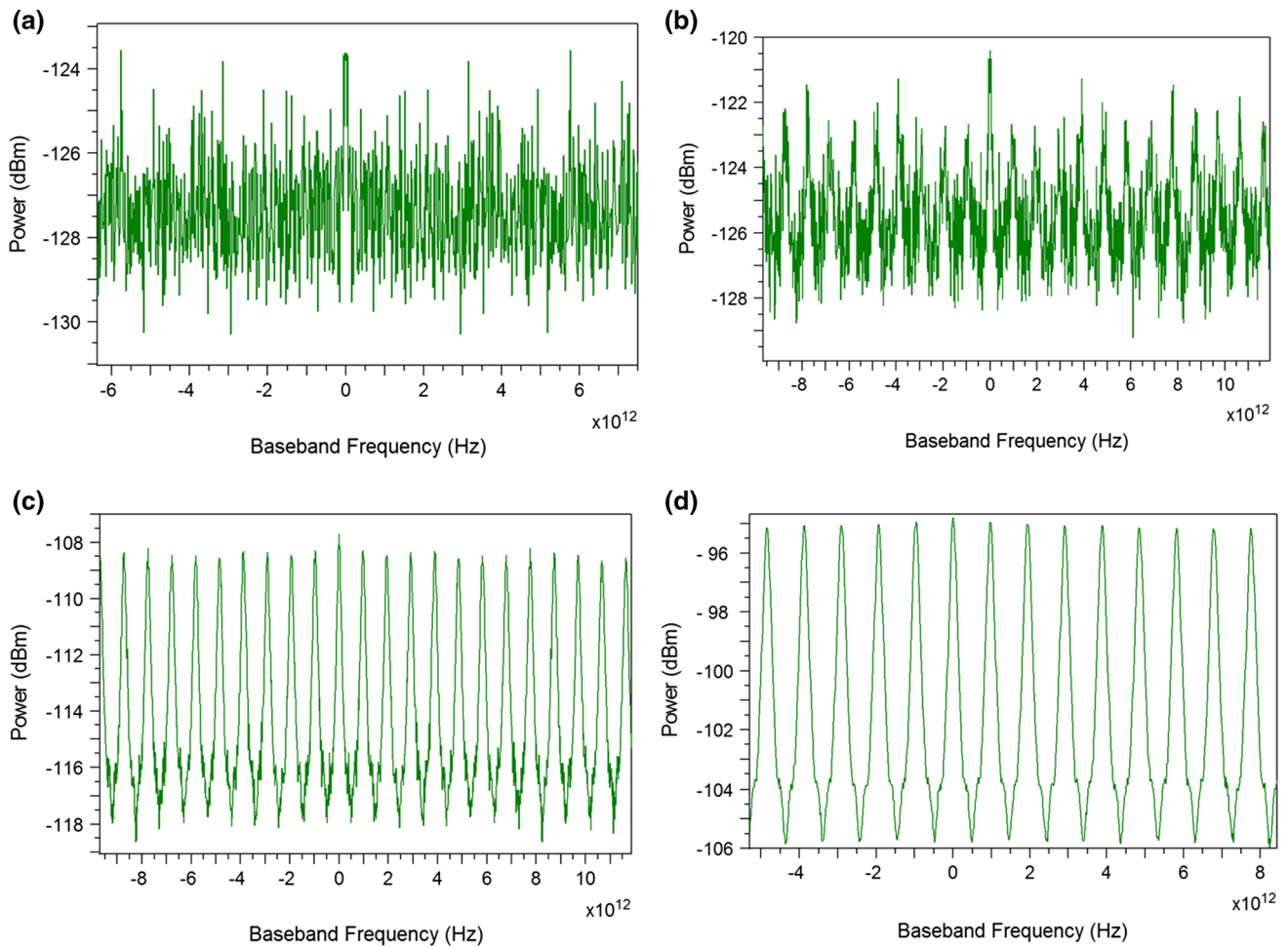
(a)

(b)

(c)

(d)

Fig. 9 Spectrum of the signal at the output of the photodetector for input power of **a** 1 mW (0 dBm), **b** 10 mW (10 dBm), **c** 100 mW (20 dBm), **d** 0.5 W (27 dBm)
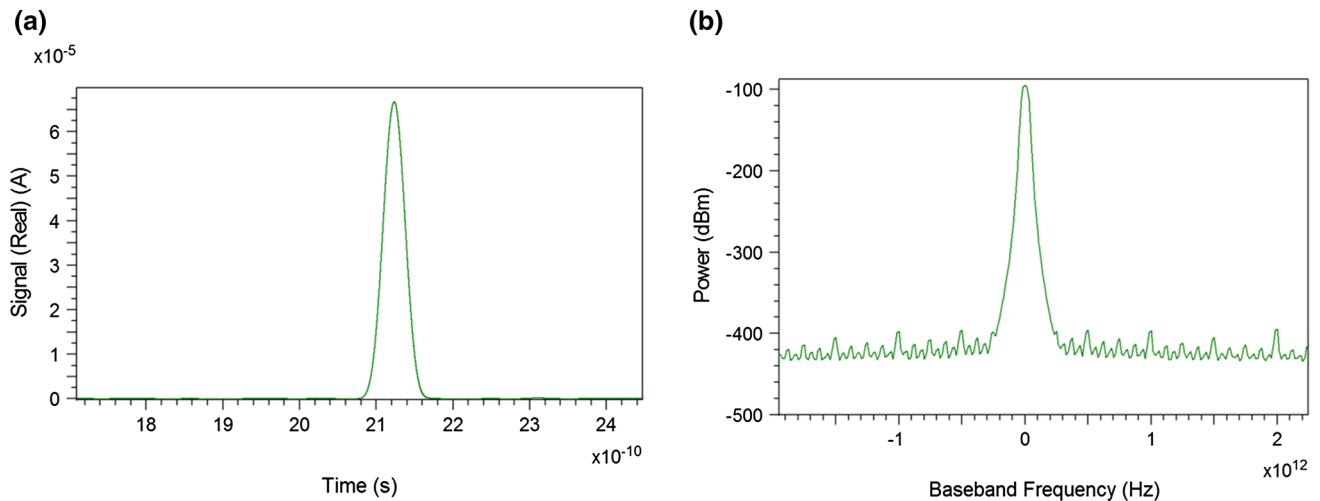
(a)

(b)

Fig. 10 Signal representation at the output of the electrical filter in **a** time domain, **b** frequency domain

The FWHM of the THz signal in time domain is found to be 0.032 ns, and the electrical power of the received signal at the output of the electrical filter is obtained as -75.69 dBm.

3.2.2 Simulation results of proposed photonic system for THz generation based on MRR and optical filter

In the second approach, an optical filter is incorporated in the proposed system for THz generation. The block schematic of the proposed photonic system for generation of THz signals in the presence of an optical filter is implemented in OptSim tool and the layout is shown in Fig. 11.

The output of MRR at the drop port consists of a series of pulses separated by the FSR. These series of pulses can be given to an optical filter in order to extract the required frequency component. The spectrum of the signal at the output of the optical filter for different resonant frequencies of the MRR is shown in Fig. 12.

The bandwidth of the optical filter is fixed at 1 nm. The type of the filter used in the simulation is an ideal optical
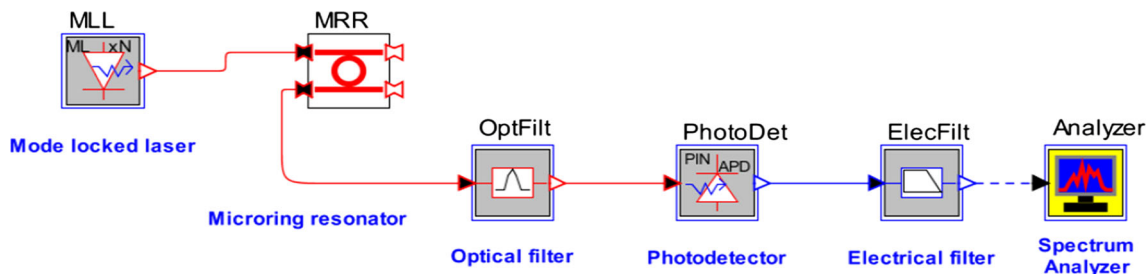

Fig. 11 Implementation of photonic system for THz signal generation in the presence of an optical filter in RSoft OptSim tool

$f_c = 1532.23$ nm

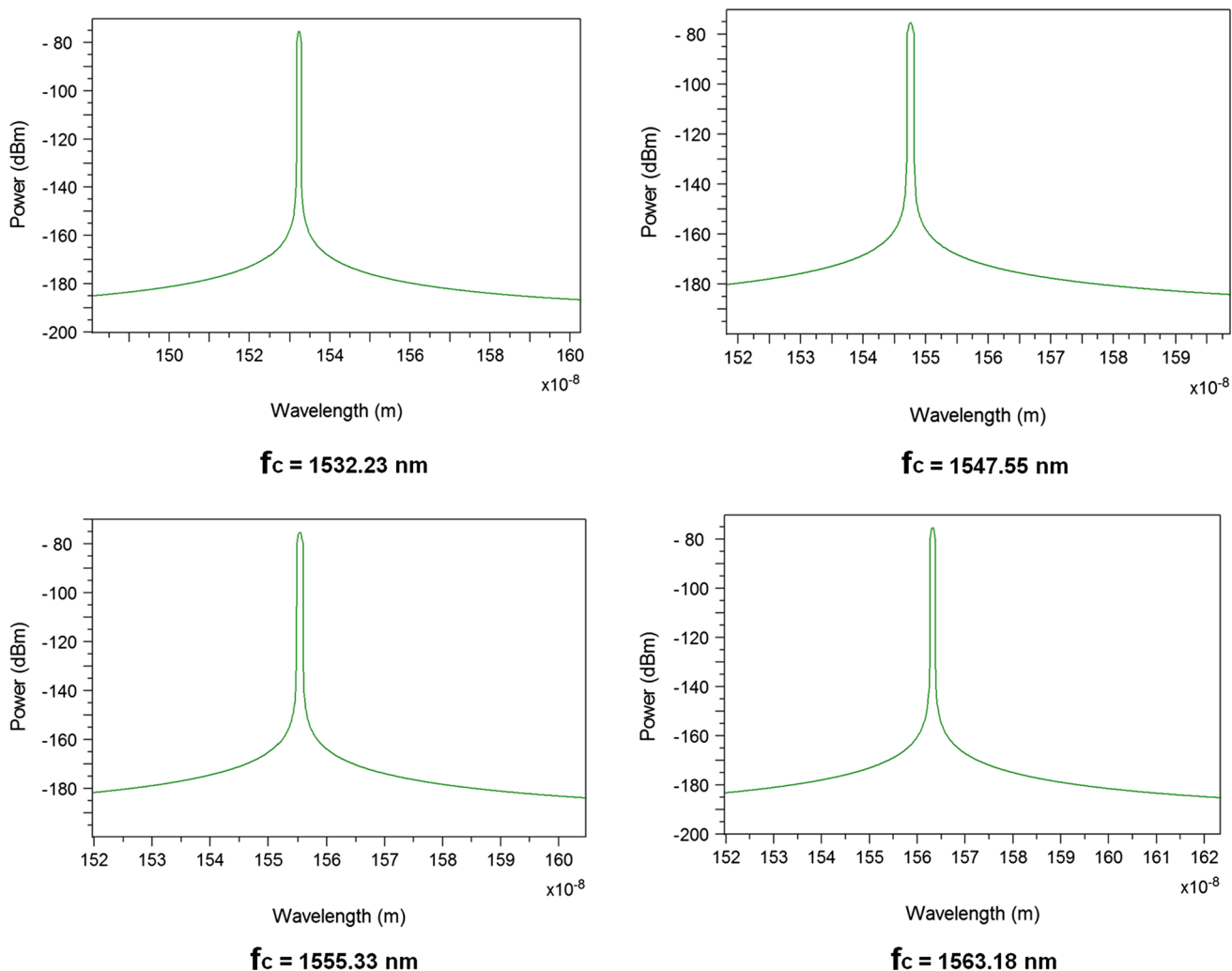$f_c = 1547.55$ nm

$f_c = 1555.33$ nm

$f_c = 1563.18$ nm

Fig. 12 Spectrum of the signal at output of optical filter for different resonant frequencies of the MRR. fc represents the center frequency of the optical filter
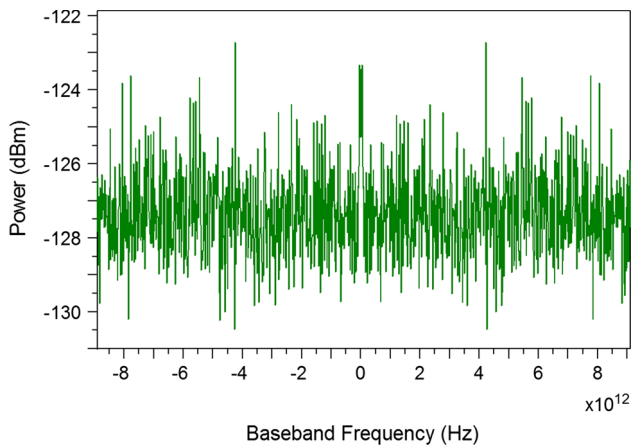
Fig. 13 Spectrum of the received signal at the output of the photodetector in the presence of an optical filter

filter whose response is unity in the band of $\lambda_0 - BW/2$ to $\lambda_0 + BW/2$, where BW is the bandwidth of the optical filter and λ_0 is the center wavelength of the optical filter. After filtering out the required optical frequency component, it is given to a photodetector to obtain the necessary THz signal in electrical domain. The spectrum of the electrical signal obtained at the output of the photodetector is shown in Fig. 13. Various types of noises affecting the quality of the received signal at the photodetector such as shot noise, dark noise, relative intensity noise (RIN) are enabled during simulations, and the effect of these noises on the received signal can be observed in Fig. 13. The value of dark current was fixed at 1 μA.

An electrical filter can be used to extract the received signal, thereby removing the noise components. The received signal at the output of the electrical filter is shown in Fig. 14. The power of the signal received at the output of the electrical filter is found to be − 109.93 dBm, and the FWHM of the
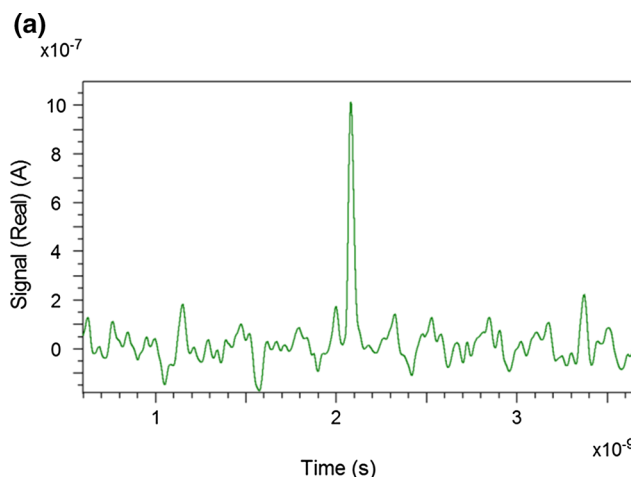
THz carrier in frequency domain and time domain is found to be 0.2618 THz and 0.053 ns, respectively.

4 Modeling of microring resonator of proposed dimensions employed in the photonic system

The microring resonator employed in the photonic system for THz signal generation is modeled in RSoft's computer-aided design (CAD) tool named FullWAVE. It is based on finite difference time domain (FDTD) algorithm to perform full vector simulation of photonic structures which can also be used for studying the propagation of light in numerous photonic structures such as waveguides, photonic crystals, etc. Silicon-on-insulator (SOI) is chosen to be the material for designing the microring resonator since it is considered to be a potential material for photonic integrated devices due to the advantages offered by it such as reduction in device dimension due to large index difference between silicon and its oxide, fabrication processes compatible to existing CMOS technology [26, 50]. The structure of the microring resonator on an SOI wafer along with the top view of the ring resonator waveguide structure is shown in Fig. 15.

The structure of the waveguide designed to model the microring resonator structure is shown in Fig. 16a. The single-mode profile of the waveguide along with the effective index profile is represented in Fig. 16b, c, respectively.

The radius of the ring resonator is 20 μm. The resonance wavelength is calculated from Eq. (1), and its value is obtained as 1555.33 nm for a radius of 20 μm. From Fig. 16c, it is found that the effective refractive index of the waveguide is 2.456 at resonance wavelength of 1555.33 nm. The width of the waveguide is 400 nm to allow single-mode propagation. The gap separation between the ring and the bus waveguide
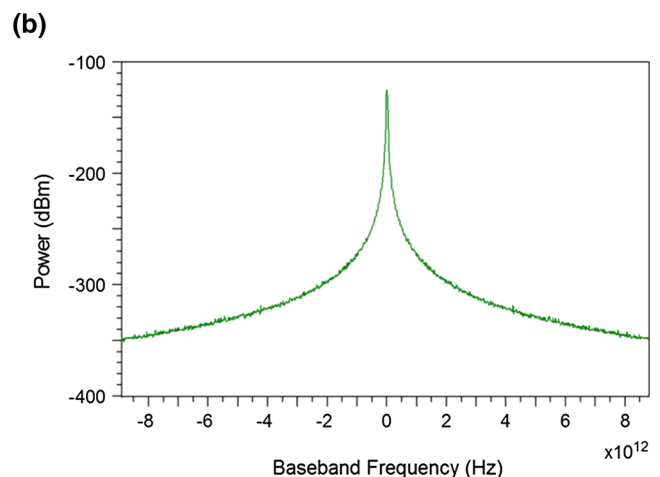
(a)

(b)

Fig. 14 Representation of the THz carrier generated at the output of the electrical filter in **a** time domain, **b** frequency domain
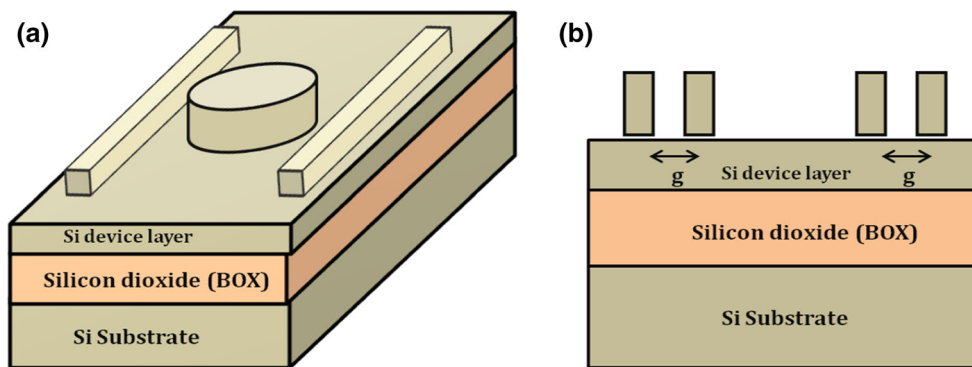
Fig. 15 **a** MRR structure on a SOI wafer, **b** top view of the MRR waveguide structure. *BOX* buried oxide, *g* gap separation between bus waveguide and ring cavity
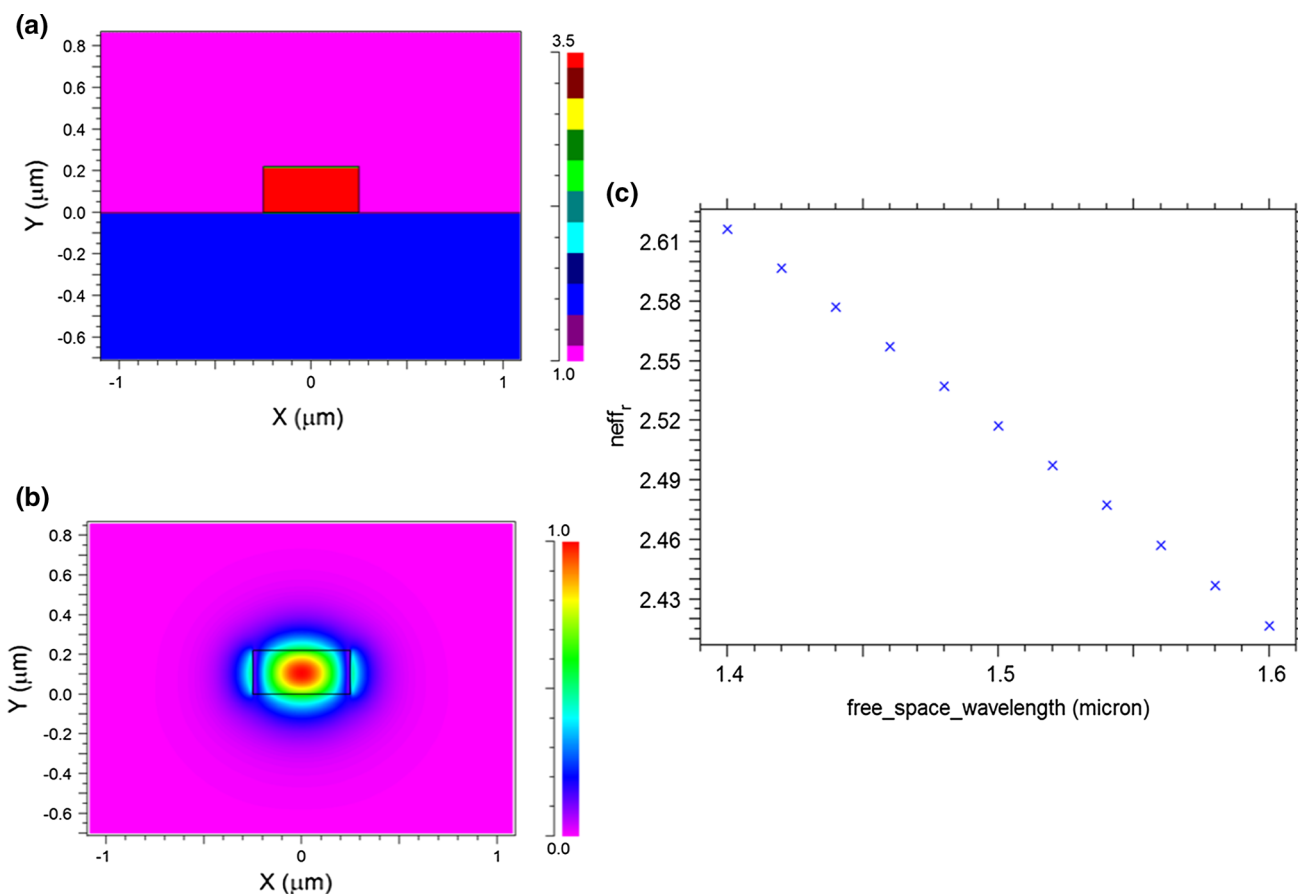

Fig. 16 **a** Top view of the waveguide structure, **b** propagation of mode through the waveguide, **c** effective index profile for different wavelengths

is 100 nm. The layout of the modeled ring resonator structure in CAD tool along with its refractive index profile is shown in Fig. 17.

The layout of the ring resonator shown in Fig. 17a is simulated in CAD tool. The grid size of the layout is fixed as 0.03, and the type of excitation is a slab mode. The propagation of electric field at ON resonance and OFF resonance is shown in Fig. 18.

It is observed from Fig. 18 that, at ON resonance, the optical signal couples into the ring and emerges at the drop port, whereas at OFF resonance condition the optical signal propagates through the bus waveguide and emerges at the through port.

The comparison between proposed work and existing literature on microring resonator-based systems for THz carrier generation has been given in Table 2.
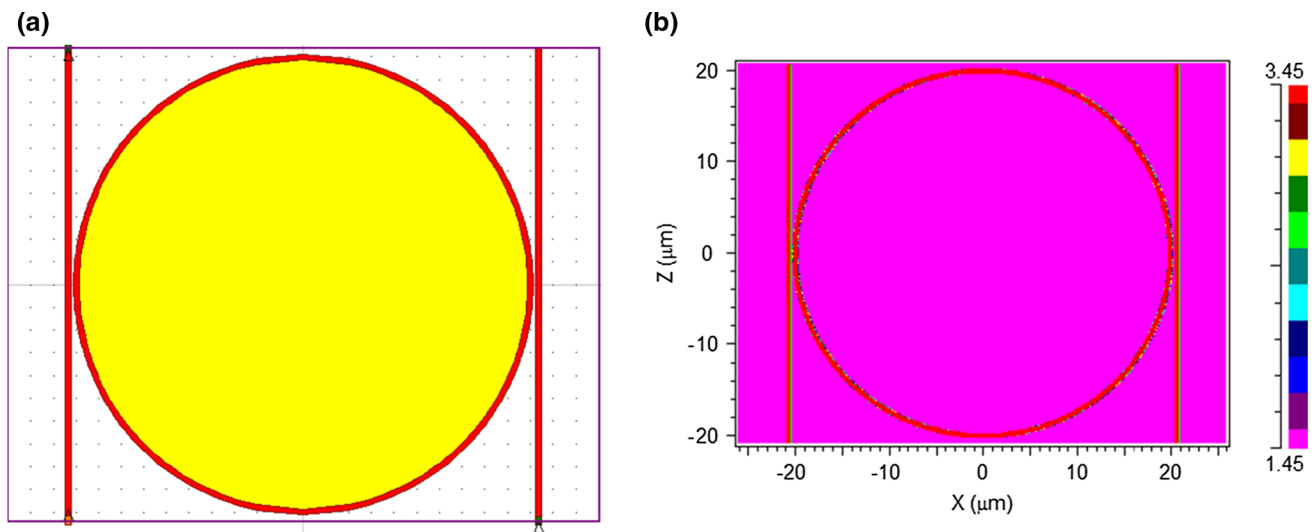
(a)

(b)

Fig. 17 **a** Layout of the ring resonator modeled in CAD tool, **b** refractive index profile of the ring resonator
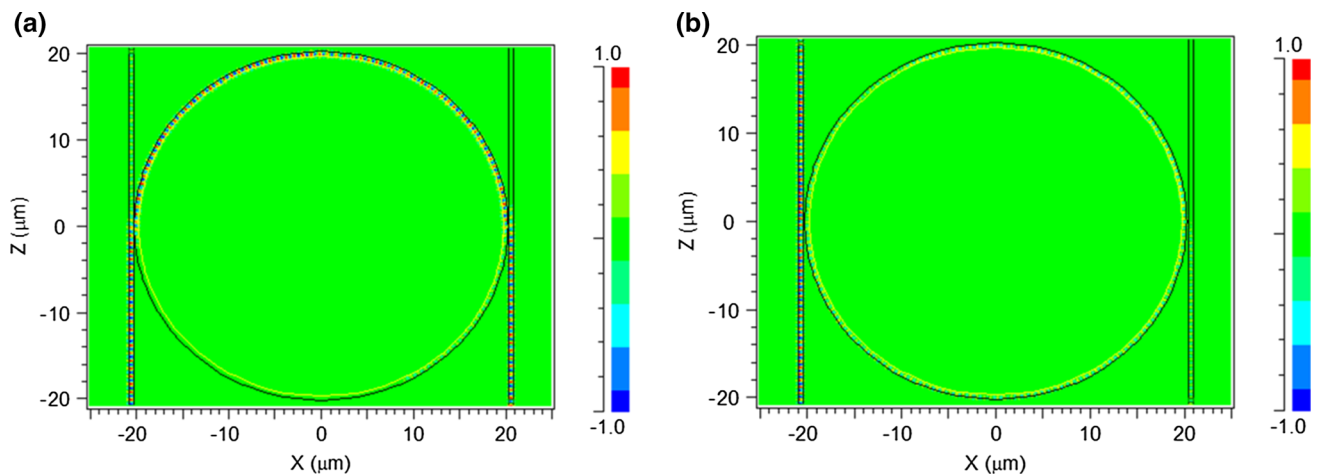
(a)

(b)

Fig. 18 Propagation of electric field through the ring resonator at **a** ON resonance, **b** OFF resonance

Table 2 Comparison between proposed system and the existing literature	References	No. of MRRs	Radius of MRR	Material used for modeling MRR	Generated frequency
	[31]	2	1.9 mm and 127 μm	SOI	25 GHz
	[32]	2	20 μm and 5 μm	InGaAsP/InP	6.29 THz
	[34]	1 (All pass configuration)	360 μm	SOI	0.5–10 THz
	Proposed system	1 (Add–drop configuration)	20 μm	SOI	1 THz

It can be observed that a compact microring resonator-based photonic system has been designed and simulated. Although the proposed system generates a comb of THz pulses with a fixed spacing of 1 THz, the compactness and the material feasibility makes the proposed system suitable for integrated photonic applications.

5 Conclusion

A novel, compact photonic system for generation of THz carriers is proposed and simulated in commercial software. The photonic system consists of only single microring resonator of 20 μm ring radius and can be easily fabricated

with the available fabrication technologies. This microring resonator is also modeled in a CAD tool. The photonic system is analyzed in two methods. Firstly, the output of the MRR is given to a photodetector which results in a train of 33 THz pulses separated by 1 THz. The resultant FWHM of the pulse obtained was found to be 0.032 ns. In the second scenario, an optical filter was employed in the photonic system after the MRR to filter a particular frequency component which is then given to a photodetector. In this case, the FWHM of the obtained THz carrier pulse is 0.053 ns. It is observed that the FWHM of the output THz carrier is higher when an optical filter is employed in the proposed system, whereas the output power of the received signal was higher in the case of the system without an optical filter. The proposed microwave photonic system generates THz carriers which can be efficiently used for communication between a pico cell or femto cell base station and the mobile user or between two devices present in the same pico/femto cell or different cells deployed in a macro cell of a 5G network.

References

[1] Seeds, A., Lee, C.H., Funk, E., Nagamura, M.: Guest editorial: microwave photonics. J. Lightwave Technol. **21**(12), 2959–2960 (2003)

[2] Seeds, A.J., Williams, K.J.: Microwave photonics. J. Lightwave Technol. **24**(12), 4628–4641 (2006)

[3] Capmany, J., Novak, D.: Microwave photonics combines two worlds. Nat. Photonics **1**(6), 319–330 (2007)

[4] Ridgway, R.W., Dohrman, C.L., Conway, J.A.: Microwave photonics programs at DARPA. J. Lightwave Technol. **32**(20), 3428–3439 (2014)

[5] Urick, V.J., Williams, K.J., McKinney, J.D.: Fundamentals of Microwave Photonics. Wiley, New York (2015)

[6] Lee, C.H.: Microwave Photonics. CRC Press, Boca Raton (2013)

[7] Xu, K., Wang, R., Dai, Y., Yin, F., Li, J., Ji, Y., Lin, J.: Microwave photonics: radio-over-fiber links, systems, and applications. Photonics Res. **2**(4), B54–B63 (2014)

[8] Capmany, J., Muñoz, P.: Integrated microwave photonics for radio access networks. J. Lightwave Technol. **32**(16), 2849–2861 (2014)

[9] Fiorani, M., Skubic, B., Mårtensson, J., Valcarenghi, L., Castoldi, P., Wosinska, L., Monti, P.: On the design of 5G transport networks. Photonic Netw. Commun. **30**(3), 403–415 (2015)

[10] Sotom, M., Bénazet, B., Le Kernec, A., Maignan, M.: Microwave photonic technologies for flexible satellite telecom payloads. In: Proceedings of the 35th European Conference on Optical Communication, Vienna, pp. 1–4 (2009)

[11] Raza, A., Ghafoor, S., Butt, M.F.U.: MIMO-enabled integrated MGDM–WDM distributed antenna system architecture based on plastic optical fibers for millimeter-wave communication. Photonic Netw. Commun. **35**(2), 265–273 (2018)

[12] Capmany, J., Ortega, B., Pastor, D.: A tutorial on microwave photonic filters. J. Lightwave Technol. **24**(1), 201–229 (2006)

[13] Nagatsuma, Tadao, Nishii, Hiroki, Ikeo, Toshiyuki: Terahertz imaging based on optical coherence tomography. Photonic Res. **2**(4), B64–B69 (2014)

[14] Manka, M.E.: Microwave photonics for electronic warfare applications. In Proceedings of IEEE International Topical Meeting on Microwave Photonics (MWP), Australia, pp. 275–278 (2008)

[15] Waterhouse, R., Novack, D.: Realizing 5G: microwave photonics for 5G mobile wireless systems. IEEE Microw. Mag. **16**(8), 84–92 (2015)

[16] Tsokos, C., Groumas, P., Katopodis, V., Avramopoulos, H., Kouloumentas, C.: Enabling photonic integration technology for microwave photonics in 5G systems. In: Proceedings of IEEE 19th International Conference on Transparent Optical Networks (ICTON), Catalonia, pp. 1–4 (2017)

[17] Nagatsuma, T., Ducournau, G., Renaud, C.C.: Advances in terahertz communications accelerated by photonics. Nat. Photonics **10**(6), 371–379 (2016)

[18] Akyildiz, I.F., Jornet, J.M., Han, C.: Terahertz band: next frontier for wireless communications. Phys. Commun. **12**, 16–32 (2014)

[19] Liu, L.: Compressed sensing on terahertz imaging. Doctoral dissertation, University of Liverpool (2017)

[20] Chen, Y., Ding, Y., Zhu, Z., Chi, H., Zheng, S., Zhang, X., Jin, X., Galili, M., Yu, X.: Photonic compressive sensing with a microring-resonator-based microwave photonic filter. Opt. Commun. **373**, 65–69 (2016)

[21] Nagatsuma, T., et al.: Terahertz wireless communications based on photonics technologies. Opt. Express **21**(20), 23736–23747 (2013)

[22] Song, H.J., Oh, K.H., Shimizu, N., Kukutsu, N., Kado, Y.: Generation of frequency-modulated sub-terahertz signal using microwave photonic technique. Opt. Express **18**(15), 15936–15941 (2010)

[23] Sun, D., Dong, Y., Yi, L., Wang, S., Shi, H., Xia, Z., Xie, W., Hu, W.: Photonic generation of millimeter and terahertz waves with high phase stability. Opt. Lett. **39**(6), 1493–1496 (2014)

[24] Carpintero, G., Hisatake, S., de Felipe, D., Guzman, R., Nagatsuma, T., Keil, N., Göbel, T.: Photonics-based millimeter and terahertz wave generation using a hybrid integrated dual DBR polymer laser. In: Microwave Symposium (IMS), 2016 IEEE MTT-S International 2016 May 22, pp. 1–3. IEEE

[25] Soltanian, M.R., Amiri, I.S., Alavi, S.E., Ahmad, H.: Dual-wavelength erbium-doped fiber laser to generate terahertz radiation using photonic crystal fiber. J. Lightwave Technol. **33**(24), 5038–5046 (2015)

[26] Bogaerts, W., De Heyn, P., Van Vaerenbergh, T., De Vos, K., Kumar Selvaraja, S., Claes, T., Dumon, P., Bienstman, P., Van Thourhout, D., Baets, R.: Silicon microring resonators. Laser Photonics Rev. **6**(1), 47–73 (2012)

[27] Feng, S., Lei, T., Chen, H., Cai, H., Luo, X., Poon, A.W.: Silicon photonics: from a microresonator perspective. Laser Photonics Rev. **6**(2), 145–177 (2012)

[28] Ehteshami, N., Zhang, W., Yao, J.: Optically tunable single passband RF tilter based on phase-modulation to intensity-modulation conversion in a silicon-on-insulator microring resonator. In: Proceedings of the 2015 International Topical Meeting on RFs (MWP), Paphos, Cyprus, 26–29 October 2015, pp. 1–4

[29] Chew, S.X., Yi, X., Yang, W., Wu, C., Li, L., Nguyen, L., Minasian, R.: Optoelectronic oscillator based sensor using an on-chip sensing probe. IEEE Photonics J. **9**, 5500809 (2017)

[30] Ehteshami, N., Zhang, W., Yao, J.: Optically tunable full 360° microwave photonic phase shifter using three cascaded silicon-on-insulator microring resonators. Opt. Commun. **373**, 53–58 (2016)

[31] Amiri, I.S., Ahmad, H., Ghasemi, M., Ismail, M.F., Aidit, S.N., Soltanian, M.R., Nafarizal, N.: Silicon-based microring resonators for multi-solitons generation for THz communication. Opt. Quant. Electron. **48**(8), 415 (2016)

[32] Luangxaysana, Khanthanou, Mitatha, Somsak, Yoshida, Masahiro, Komine, Noriyuki, Yupapin, Preecha P.: High-capacity terahertz carrier generation using a modified add-drop filter for radio frequency identification. Opt. Eng. **51**(8), 085006 (2012)

[33] Amiri, I.S., Alizadeh, F., Ariannejad, M.M., Amini, R., Yupapin, P.: Computation of ion exchange buried microring resonator waveguide for THz communication applications. Results Phys. **10**, 287–290 (2018)

[34] Sinha, R., Karabiyik, M., Al-Amin, C., Vabbina, P.K., Güney, D.Ö., Pala, N.: Tunable room temperature THz sources based on nonlinear mixing in a hybrid optical and THz micro-ring resonator. Sci. Rep. **5**, 9422 (2015)

[35] Furusawa, K., Sekine, N., Kasamatsu, A., Uzawa, Y.: Microring resonator based frequency comb sources for compact continuous-wave THz generators. In: Proceedings of IEEE 42nd International Conference on Infrared, Millimeter, and Terahertz Waves (IRMMW-THz), Cancum, pp. 1–2 (2017)

[36] Lo, M.C., Guzmán, R., Gordón, C., Carpintero, G.: Mode-locked laser with pulse interleavers in a monolithic photonic integrated circuit for millimeter wave and terahertz carrier generation. Opt. Lett. **42**(8), 1532–1535 (2017)

[37] Huff, L.: Optics to enable 5G Mobile Networks, Blog of 2018 Optical Fiber Communication Conference, https://www.ofcconference.org/en-us/home/about/ofc-blog/2018/march-2018/optics-to-enable-5g-mobile-networks/

[38] Liu, Cheng, Wang, Jing, Cheng, Lin, Zhu, Ming, Chang, Gee-Kung: Key microwave-photonics technologies for next-generation cloud-based radio access networks. J. Lightwave Technol. **32**(20), 3452–3460 (2014)

[39] Chandrasekhar, V., Andrews, J.G., Gatherer, A.: Femtocell networks: a survey. IEEE Commun. Mag. **46**(9), 1–23 (2008)

[40] Niu, Y., Li, Y., Jin, D., Su, L., Vasilakos, A.V.: A survey of millimeter wave communications (mmWave) for 5G: opportunities and challenges. Wireless Netw. **21**(8), 2657–2676 (2015)

[41] Rodriguez, J.: Fundamentals of 5G Mobile Networks. Wiley, London (2015)

[42] Shams, Haymen, Seeds, Alwyn: Photonics, fiber and THz wireless communication. Opt. Photonics News **28**(3), 24–31 (2017)

[43] Smith, P.W.: Mode-locking of lasers. Proc. IEEE **58**(9), 1342–1357 (1970)

[44] Menzel, R.: Photonics, Linear and Nonlinear Interactions of Laser Light and Matter. Springer, New Delhi (2004)

[45] Rabus, D.G.: Integrated Ring Resonators: The Compendium. Springer, Heidelberg (2007)

[46] Chen, Y.F., Chang, M.T., Zhuang, W.Z., Su, K.W., Huang, K.F., Liang, H.C.: Generation of sub-terahertz repetition rates from a monolithic self-mode-locked laser coupled with an external Fabry-Perot cavity. Laser Photonics Rev. **9**(1), 91–97 (2015)

[47] Obraztsov, P.A., Okhrimchuk, A.G., Rybin, M.G., Obraztsova, E.D., Garnov, S.V.: Multi-gigahertz repetition rate ultrafast waveguide lasers mode-locked with graphene saturable absorbers. Laser Phys. **26**(8), 084008 (2016)

[48] Hou, Lianping, Haji, Mohsin, Marsh, John H.: Mode-locking and frequency mixing at THz pulse repetition rates in a sampled-grating DBR mode-locked laser. Opt. Exp. **22**(18), 21690–21700 (2014)

[49] Niigaki, R., Kida, Y., Imasaka, T.: Mode-locked laser with a repetition rate of 17.6 THz. Appl. Opt. **56**(27), 7636–7641 (2017)

[50] Vorckel, A., Monster, M., Henschel, W., Bolivar, P.H., Kurz, H.: Asymmetrically coupled silicon-on-insulator microring resonators for compact add-drop multiplexers. IEEE Photonics Technol. Lett. **15**(7), 921–923 (2003)

Rohan Katti received his Master's degree in Communication Systems from SRM Institute of Science and Technology in 2015. He is currently pursuing his Ph.D. in the department of Electronics and Communication Engineering, SRM Institute of Science and Technology under the Visvesvaraya Ph.D. Scheme funded by the Ministry of Electronics and Information Technology (MeitY), Government of India. His research interests include silicon photonics, photonic device modeling, microwave photonics, reversible logic circuit design in optical domain.

Shanthi Prince is a Professor in the department of Electronics and Communication Engineering, SRM Institute of Science and Technology. Her research interests include diffuse reflectance spectroscopy studies on tissues, development of noninvasive instrumentation for biomedical applications, underwater optical wireless communication, optical wireless channel modeling, passive optical networks, all optical processing, Visible light communications. She has published several papers in reputed journals and is the author of a book, four book chapters and co-author of three book chapters. She is the recipient of IETE-CEOT award for the contributions in the field of Biophotonics for the year 2016 and the recipient of Dr. A. P. J. Abdul Kalam Inspiring Teacher Award instituted by IET CLN for the year 2014–2015. She is currently working on research projects funded by DRDO and ISRO, Government of India.